Dynamics of front-like water evaporation phase transition interfaces

V.A. Shargatov[a,b], S.V. Gorkunov[a,b], A.T. Il'ichev[c,d,*]

[a] *Ishlinsky Institute for Problems in Mechanics RAS, Vernadskogo pr., 101, Moscow 119526, Russia*
[b] *National Research Nuclear University MEPhI, Kashirskoye shosse 31, Moscow 115409, Russia*
[c] *Steklov Mathematical Institute, Russian Academy of Sciences, Gubkina 8, Moscow 119991,Russia*
[d] *Bauman Moscow Technical University, Baumanskaya str. 5, Moscow 105110, Russia*

Abstract

We study global dynamics of phase transition evaporation interfaces in the form of traveling fronts in horizontally extended domains of porous layers where a water located over a vapor. These interfaces appear, for example, as asymptotics of shapes of localized perturbations of the unstable plane water evaporation surface caused by long-wave instability of vertical flows in the non-wettable porous domains. Properties of traveling fronts are analyzed analytically and numerically. The asymptotic behavior of perturbations are described analytically using propagation features of traveling fronts obeying a model diffusion equation derived recently for a weakly nonlinear narrow waveband near the threshold of instability. In context of this problem the fronts are unstable though nonlinear interplay makes possible formation of stable wave configurations. The paper is devoted to comparison of the known results of front dynamics for the model diffusion equation, when two phase transition interfaces are close, and their dynamics in general situation when both interfaces are sufficiently far from each other.

Keywords: Porous medium, Evaporation, Interface, Turning point bifurcation, Front stability, Fingering, KPP equation

1. Introduction

We treat a particular class of flows in a porous medium that are subjected to a transition to instability via a zero critical wave number. These are flows in extended horizontal domains of porous media with a phase transition occurring on some interface within the flow region. As an example, we may consider

*Corresponding author
Email addresses: shargatov@mail.ru (V.A. Shargatov), gorkunov.ser@mail.ru (S.V. Gorkunov), ilichev@mi.ras.ru (A.T. Il'ichev)

a model describing filtration processes in natural massifs, having contact with mines, tunnels and other constructions. The functioning of such engineering systems is accompanied by heat and mass exchange between the construction and surrounding rock [1]. Artificial ventilation makes it possible to keep the microclimate, necessary for exploitation. Ventilation is accompanied by evaporation from a ceiling of the construction while the ground water moves downwards under the action of gravity or pressure in the water horizon. The water can enter the underground construction either in liquid or vapor states. If the surrounding rock has relatively low permeability it is natural to assume that the underground water moving towards the ceiling of the construction evaporates somewhere in a porous space and diffuses into the underground construction as a vapor. In this case a region saturated with a blend of vapor and air arises between the free space and the water saturated region.

For the transition with the most unstable mode of infinite length (zero wave number) as the perturbations grow monotonically, the evolution of the narrow band of weakly nonlinear modes near the instability threshold is described by a diffusion Kolmogorov-Petrovskii-Piskounov-Fisher (KPP) equation with a non-degenerate quadratic nonlinearity in the generic case (see [2]). This kind of equation was first considered in [3] to describe an increase in the amount of substance as applied to a biological problem. It has some interesting properties, which have been discussed in numerous publications (see, e.g., [4],[5] and references therein).

It has been shown that, if the porous medium is nonwettable, there can be two or none stationary plane phase transition interfaces. At the zero wave number, the stability margin is reached simultaneously with the vanishing of the solution to the stationary problem [2]. As was mentioned the dynamics of the system in question near the instability threshold is described by the KPP equation. In this case both phase transition interfaces are located close to each other.

The model studied below provides the possibility of detecting fundamental physical effects of an evolution of perturbations of the vertical base flow between the existing phase transition interface close to and far away from the instability threshold. Conceptually, this work continues the study performed in [6]. More specifically, in [6] we treat the evolution of localized finite perturbations of the basic flow. In this case, numerical methods are required and, along with the study of physical effects, we can determine the limits of applicability of the fundamental results obtained in [2] for the case of finite amplitude localized perturbations, i.e. for problems of practical importance.

Perturbation of the phase transition interfaces of the base flow separating a fluid and vapor, plays a particular role because they are solutions of the base system of equations and, hence, any perturbation of them has to tend asymptotically to these surfaces. Dynamics of surfaces initially separating the fluid and vapor was investigated in [7]. It was shown that they tend either to stable base interface, or the highest boundary of the reservoir, depending on their initial location.

The present paper deals with a description of dynamics of fronts in the full

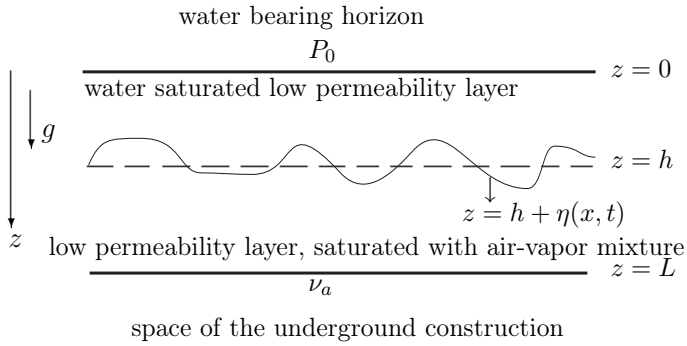

Figure 1: Schematic of the system considered; see text for definitions

model, which may appear, for example, due to long-time evolution of a localized perturbation of the upper unstable front. In this case, the perturbation remaining localized has increasing support. Its lateral boundaries after some time propagate as traveling fronts. In case when the stable and unstable interfaces are close and the KPP equation describes such a configuration these traveling fronts are corresponding solutions of this equation. We discuss stability of these solutions and also possibility of existence of similar solutions when the phase transition interfaces are not close (the system is far from the threshold of instability).

The paper is organized as follows. In Sec. 2 we give the formulation of the problem, in Sec. 3 we recall the dynamics of initial horizontal interfaces and also the basic KPP equation describing the dynamics of the system near the threshold of instability. In Sec. 4 we make a comparative analysis of the known propagation properties of front solutions of the model KPP equation describing the dynamics of the system near the threshold of instability and their properties in general case, when the phase transition interfaces are not close. We show that KPP fronts well describe the situation in general case. Sec. 5 is devoted to discussion of stability properties in the case of close phase transition interfaces when the fronts have the oscillatory structure (which is possible in our model). In Sec. 6 we give our conclusions.

2. Dynamics of the system

Let the high permeability water horizon with the water pressure P_0, bounded from above by the plane $z = 0$, be located over the ceiling $z = L$ (the z-axis is directed downwards). The rock in a layer $0 < z < L$ has a low permeability and at the surface $z = L$ it is streamlined by air of humidity ν_a which is smaller than the humidity of saturation, i. e. the partial pressure in the air is smaller than the pressure of saturation of the vapor in the air at a given value of temperature T. In this case the low permeability porous media $0 < z < L$ contains the

water layer $0 < z < h$ and the layer $h < z < L$, saturated by a mixture of the air and water vapor (Fig. 1) and is adjacent to the space of the underground construction $z > L$ (see Fig. 1). The x-axis is directed horizontally.

Assuming the fluids to be incompressible we get the continuity equation and Darcy's law as the governing equations in the water saturated domain

$$\mathrm{div}\mathbf{v}_w = 0, \qquad \mathbf{v}_w = -\frac{k}{\mu_w m}\ \mathrm{grad}\ (P - \rho_w g z). \tag{1}$$

The governing equations in the domain saturated by the air-vapor mixture represents the equation of vapor diffusion and the Clapeyron equation for gases:

$$\frac{\partial \rho_v}{\partial t} = \mathrm{div}\ D\mathrm{grad}\ \rho_v \quad P_v = \rho_v R_v T, \quad P_a = \rho_a R_a T. \tag{2}$$

Here $\mathbf{v}_w$ is the water velocity, m is porosity, k is the permeability, μ is the viscosity, P is the pressure, g is the gravity, ρ is the density, T the temperature, D is the diffusion coefficient. Typical values are (see e. g. [8]) $D = 2.4 \times 10^{-5}$ $\mathrm{m^2 s^{-1}}$, $P_a = 10^5$ Pa, $R_a = 287$ J $\mathrm{kg^{-1} K^{-1}}$, $R_v = 461$ J $\mathrm{kg^{-1} K^{-1}}$.

The subscripts v, w and a correspond to the vapor, water and air, respectively. Instead of the equation for the vapor density it is convenient to use the analogous equation for the humidity function $\nu = \rho_v/(\rho_a + \rho_v)$. This equation follows from (2) under the condition of smallness of the partial pressure of the vapor in comparison with the atmospheric pressure [8]:

$$\frac{\partial \nu}{\partial t} = D\ \Delta\nu. \tag{3}$$

The system of equations (1) is reduced to the Laplace equation

$$\Delta\ P = 0. \tag{4}$$

The boundary condition at the front for a pressure jump reads

$$P_w = P_v + P_c \equiv P_a + P_c. \tag{5}$$

Here the capillary pressure P_c is negative, when the rock is wettable and it is positive for the non-wettable rock. The boundary condition for the humidity at the front follows from the definition of the humidity function and Clapeyron's equations for the air and vapor:

$$\nu = \nu_* = \frac{R_a}{R_v}\frac{P_{v*}}{P_a}, \quad z = h. \tag{6}$$

From the assumption that the processes under consideration are isothermal it follows that the humidity on the front being a function of the temperature is a constant in the framework of our model. The water mass conservation law at the front takes the form [2]

$$\left(1 - \frac{\rho_v}{\rho_w}\right)\mathbf{V}_n = -\frac{k}{m\mu_w}\left[\ \mathrm{grad}\ (P - \rho_w g z)\right]_n + D\frac{\rho_a}{\rho_w}\left(\ \mathrm{grad}\ \nu\right)_n, \quad z = h. \tag{7}$$

The boundary condition at the upper boundary $z = 0$ and at the lower boundary, coinciding with the ceiling are written as

$$z = 0: \quad P = P_0; \quad z = L: \quad \nu = \nu_a. \tag{8}$$

The processes under consideration are characterized by the physical parameters which determine the dimensionless quantities

$$\alpha = \frac{P_c + P_a - P_0}{\rho_w g L}, \qquad \beta = \frac{D}{k}\frac{\rho_a}{\rho_w}\left(\nu_* - \nu_a\right)\frac{m\mu_w}{\rho_w g L}, \tag{9}$$

playing the considerable role in further observations. We note, that the parameter α in (9) is the measure of deviation of the pressure P_0 in the aquifer from the hydrostatic one for the given value of the capillary pressure, and the parameter β characterizes the ratio between the rate of the diffusion transfer of the vapor and the rate of the water flux, caused by the hydrostatic pressure.

From (2)-(8) the expressions for the distribution of pressure and humidity in the layers $0 < z < h$ and $h < z < L$ follow:

$$P_{st} = P_0 + \frac{P_a + P_c - P_0}{h}\, z, \qquad \nu_{st} = \frac{\nu_a - \nu_*}{L - h}\, z + \frac{L\nu_* - h\nu_a}{L - h}, \tag{10}$$

and also the equation for the location of the evaporation front:

$$\frac{\alpha}{H} - 1 + \frac{\beta}{1 - H} = 0, \quad H = \frac{h}{L}. \tag{11}$$

The quadratic equation (11) has the roots

$$H_{s,u} = -\frac{1}{2}\left(\beta - \alpha - 1\right) \pm \frac{1}{2}\sqrt{\left(\beta - \alpha - 1\right)^2 - 4\alpha}, \quad H_s \geq H_u. \tag{12}$$

It can be easily seen that for the neutral ($P_c = 0$) or the wettable ($P_c < 0$) porous media, when $\alpha < 0$, one root of (12) is positive, and the other is negative. The physical sense has only positive root, corresponding to the sign "+" at the radical in (12).

Solution (10) describes the stationary process of evaporation on the phase transition front when the heavier fluid (water) is located above the lighter one (air-vapor blend). In the case when there exists the unique location for the stationary front of phase transition it is stable and it is evident that this solution describes the penetration of the moisture in the underground construction as a result of the vapor diffusion through the rock. This is in the case of surrounding wettable rock. If the surrounding rock is nonwettable, from results of [2] it follows, that

1. In a certain domain of parameters there exist two positive roots (12): for $P_c > 0$ the smallest root can become positive, when the pressure P_0 at the aquifer decreases in a way that α becomes positive. For the further decrease of P_0 the parameter α attains the critical value

$$\beta = \left(1 - \sqrt{\alpha}\right)^2.$$

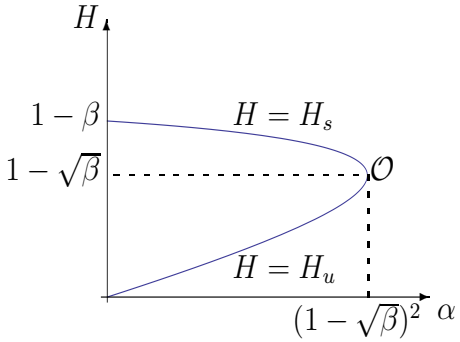

Figure 2: Bifurcation diagram H versus α at a fixed β in (9); $H = H_s$ is the stable branch, $H = H_u$ the unstable branch, $\mathcal{O}$ is the turning point

At this value the coincidence of the roots of (12) takes place, and the stationary solution (10) ceases to exist, when α exceeds this critical value (see Fig. 2).

2. If two locations of equilibrium positions of the phase transition front are possible, i. e. the both roots of (11) are positive, the lowest one of them is always dynamically unstable with respect to longwave perturbations and the larger one is stable with respect to these perturbations. The condition of loss of dynamical stability of the larger stable front coincides with the loss of existence of both fronts (turning point $\mathcal{O}$ in Fig. 2).

If the Cauchy data correspond to horizontal plane surfaces, separating the water and air from results of [7] we have

1. When the initial surface is located above the unstable phase transition interface $z = H_u$ (recall that the z-axis is directed downwards) it then moves towards the upper boundary of the low-permeability layer and reaches it at the finite time.

2. When the initial horizontal plane surface is located either between two interfaces or under the lowest stable one it tends to this stable interface.

The dynamics of these interfaces is described in details in [7]. Though, there is one more possibility, when an initial interface coincides with the lowest unstable phase transition front. In this case it doesn't move elsewhere, but the dynamics of its localized perturbation has its own features to be described in the forthcoming sections.

3. Case of close phase transition fronts.

To describe secondary structures, bifurcating from the base state (10) in a small neighborhood of the instability threshold for the mentioned type of instability we repeat here briefly the derivation of the KPP equation. Taking into account the long-wave nature of instability determine the small dimensionless parameters ϵ and ε:

$$\epsilon = L^2/l^2, \quad \varepsilon = \eta_a/L,$$

where l and η_a are characteristic values of wave length and amplitude. Determine the dimensionless variables (keeping the old notations)

$$x \to lx, \quad t \to \frac{L^2}{D}t, \quad \eta \to \eta_a \eta, \quad z \to Lz.$$

It is shown in [2] that if we put $\epsilon = \varepsilon$ we get the equation

$$c_0 \partial_\tau \eta = c_1 \eta + c_2 \partial_{xx} \eta + c_3 \eta^2, \quad \tau = \varepsilon t \tag{13}$$

Here

$$c_0 = \left(1 - \frac{\rho_a}{\rho_w}\frac{\nu_a - \nu_*}{3}\right) > 0, \quad c_1 = \varepsilon^{-1}\left(\frac{k}{D\mu_w m}\frac{P_a + P_c - P_0}{H^2} + \frac{\rho_a}{\rho_w}\frac{\nu_a - \nu_*}{(1-H)^2}\right),$$

$$c_2 = -\frac{1}{3}\left(\frac{k}{D\mu_w m}(P_a + P_c - P_0) + \frac{\rho_a}{\rho_w}(\nu_a - \nu_*)\right) > 0, \quad c_3 = -\left(\frac{k}{D\mu_w m}\frac{P_a + P_c - P_0}{H^3} + \frac{\rho_a}{\rho_w}\frac{\nu_* - \nu_a}{(1-H)^3}\right) < 0.$$

Because of the condition of the marginal stability [2], the coefficient c_1 is of order 1 in a neighborhood of the marginal stability.

By the use of the appropriate scaling equation (13) may be reduced to the standard KPP form (the old notations are kept)

$$\partial_\tau \eta = \eta - \eta^2 + \partial^2_{xx}\eta, \tag{14}$$

where $\eta = 0$ is the upper unstable phase transition front and $\eta = 1$ is the stable front.

4. Comparison of properties of traveling wave solutions of the KPP equation and of the full problem

4.1. Traveling fronts of the KPP equation

Evolution of a localized perturbation of the unstable phase transition interface $\eta = 0$ directed downwards can be subdivided into two following stages. The scheme of its development is given in Fig.3

Stage 1. *A*. Tendency to the stable front $\eta = 1$ until a top of the perturbation doesn't get to some vicinity of it.

Stage 2. *B*. Propagation of the perturbation (especially its lateral boundaries).

The first stage was described in details for the general case in [6] and we do not repeat it here.

Left *sl* and right *sr* lateral boundaries of any localized perturbation in a process of its evolution beginning with the moment $\tau = \tau^*$ of the origin of a second stage (*B* in Fig. 3) correspond to connections between two stationary points $\eta = 0$ and $\eta = 1$ of Eq. (14. It was obtained in [3]) that

1. Arbitrary Cauchy data $\eta_0 = \eta(x, 0)$ of $0 \le \eta_0 \le 1$ determines a unique solution of (14) satisfying the same condition.

2. Initial data

$$\begin{cases} \eta_1 = 1, & x < a, \\ \eta_1 = 0, & x > b \ge a \end{cases}$$

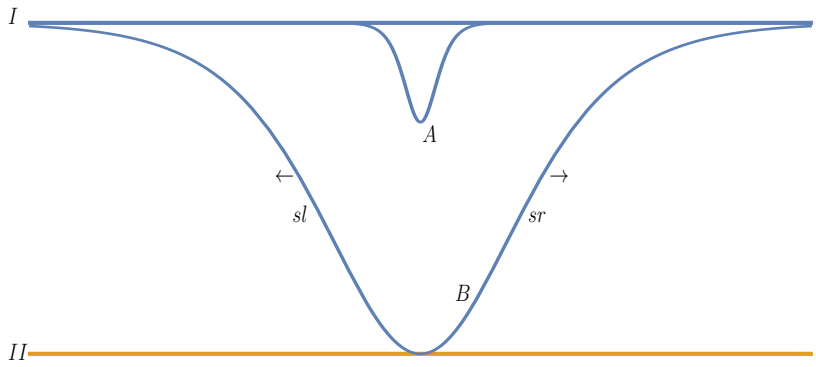

Figure 3: Schematic development of the unstable interface perturbations (I) in a vicinity of the instability threshold. A is a perturbation during a first stage, B is the perturbation at the beginning of the second stage of its development; II is the stable interface, sl and sr are lateral sides of the perturbation, arrows show the direction of propagation

translate to the left when τ grows. The shape of the curve $\eta = \eta(x, \tau)$ tends to the shape of the traveling front structure $\eta = \eta_{W_0}(x - W_0\tau)$ propagating to the right with the speed $W_0 = 2$ and satisfying to the equation

$$-W_0\eta'_{W_0} = \eta''_{W_0} + \eta_{W_0} - \eta^2_{W_0}.$$

if this front solution is stable. Here prime denotes differentiation with respect to the variable $\xi = x - W_0\tau$

Moreover, the equation

$$-W\eta'_W = \eta''_W + \eta_W - \eta^2_W. \tag{15}$$

where now $\xi = x - W\tau$ has front solutions with a structure for any $W \geq W_0 = 2$. In other words the front η_{W_0} having the speed W_0 is the limiting one having the minimal speed. Therefore, the following Proposition takes place.

Proposition 4.1 [4]. For any $W \geq W_0$ equation (15) has front solutions, monotonously tending to the asymptotes $\eta = 0$ and $\eta = 1$. Moreover, for $c = \pm\frac{5\sqrt{6}}{6}$ the front solution can be found in the explicit analytic form [9, 10].

In [5] (see, also [11]) the second stage of evolution of a localized perturbation of the unstable front was illustrated (see Fig. 7 in [5]). It can be seen, that for increasing time the lateral bounds sl and sr (Fig. 3 of the present paper) transforms into the fronts traveling with the minimal speed to the left (with the speed $-W_0$) and to the right, correspondingly.

4.2. Traveling fronts of the full problem

We examine the evolution of similar perturbations for the case of the full problem (3)-(8) when the stable and unstable interfaces are not close. The

problem has to be attacked with the help of numerical calculations. The numerical calculation includes the solution of the elliptic equation in the region with a moving boundary and the solution of the equation of the interface motion. When solving the elliptic equation, the key point is the accuracy of calculating the pressure gradient at the moving boundary because it determines the normal velocity of the contact surface. The moving boundary complicates the calculation because the computational domain changes with time. In addition, the calculation of the position of the contact surface even at a known normal speed is an algorithmically time-consuming task, especially in the case of rapidly growing short-wave perturbations, that can change the topology of the computational domain. When developing the calculation algorithm, the focus is on the accuracy of calculating the evolution of the interface.

The problem is solved numerically using the boundary element method. For this solution, the boundary of the water-saturated region is represented by a polygonal line consisting of sections-panels. Each panel is associated with the source of the potential of the double layer the density of intensity of which is determined by solving a system of linear equations for each panel. These linear equations are obtained under the assumption that the potential created by all panels in the middle of each of the panels is equal to the pressure at this point. The numerical method is described in detail in [6], and it was used in [7]. This method allows one to describe reliably and in detail the evolution of the boundary water-saturated region under a considerable deformation.

The calculation results are given below in dimensionless variables (here the coordinates x, z and the time t as in (13))

$$X = x/\sqrt{\epsilon}, Z = z, T = t.$$

To compare the results obtained in the weakly nonlinear approximation with the results of the numerical solution of the full system of equations, we consider the case when the assumptions made in the derivation of the weakly nonlinear approximation are fulfilled. If $\alpha = 0.05080158$ and $\beta = 0.6$, then the stationary solution for the plane phase transition front exists at $H_u = 0.2234$ $H_s = 0.2273$ [12]. Specify the front profile at the initial moment by the formula

$$\widetilde{\eta} = H_u + (H_s - H_u)(1 + \exp(-(X - X_0)/1.43)^{-2}.$$

The position of the front at $X_0 = -15$ is shown in Fig. 4. Such a front profile in coordinates x, τ (now and further we mean by this notation the corresponding coordinates as in (14)) corresponds to the analytical solution of equation (14) [9, 10] . This solution is a traveling wave with a speed equal to $5/\sqrt{6}$. Note, that

$$\widetilde{\eta} = \left(\frac{\alpha}{{H_u}^2} + \frac{\beta}{(1 - H_u)^2}\right)\left(\frac{\alpha}{{H_u}^3} + \frac{\beta}{(1 - H_u)^3}\right)^{-1} \eta,$$

In Fig. 5 the dependence of $\partial\widetilde{\eta}/\partial T$, obtained by numerical solution of the complete system of equations (solid line) and by equation (14) (recalculated with the help of (4.2), dashed line) is shown.

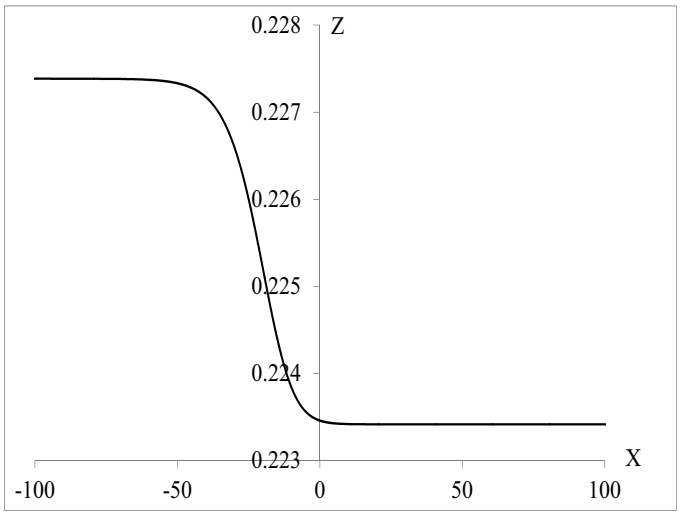

Figure 4: The shape of the front.

Now we choose the values of α and β so that the condition $(H_s - H_u) \ll 1$ remains valid, but the condition $(H_s - H_u)/H_u \ll 1$ was not fulfilled. According to [12] at $\alpha = 0.05$ and $\beta = 0.6$ there are two stationary positions of the plane front, which correspond to dimensionless Z-coordinates $H_u = 0.2053$ and $H_s = 0.2450$ and $(H_s - H_u)/H_u \approx 0.19$. The main flow with the front position H_s is stable with respect to infinitesimal perturbations, and the flow with the front position H_u is unstable if the wavelength $l > l_l$. The threshold value $l_l \approx 5.37$ is determined from the dispersion relation given in [12]. We consider the case when the main flow corresponds to the upper unstable equilibrium position of the plane front H_u. Set the initial perturbation of the front as

$$\eta = \begin{cases} H_u & \text{if } X < -l_p \\ H_u + A(1 - X/l_p)^4(1 + X/l_p)^4 & \text{if } -l_p \le X \le l_p \\ H_u & \text{if } X > l_p. \end{cases}$$

Let at the initial moment the perturbation has a width of $2l_p = 10$ and an amplitude $A = 0.1$. The perturbation width at the initial moment is greater than l_l, so the perturbation amplitude immediately begins to grow, and its effective width increases, as shown in Fig. 6.

From Fig. 6 it can be seen that the top of the perturbation $\widetilde{\eta}_{max} \to H_s$ at $T \to \infty$ and the perturbation itself takes the form of two waves spreading to the left and right, and at the time $T = 2.16 \cdot 10^6$ the speed of these waves $W_{full} \approx 1.21 \cdot 10^{-5}$.

If at the initial moment the form of the front is given by the expression

$$\widetilde{\eta} = \begin{cases} H_u + (H_s - H_u)(1 + \exp(-(X - X_0)/1.767)^{-2} & \text{if } X \le X_0 + 3.4 \\ H_u & \text{if } X > X_0 + 3.4, \end{cases}$$

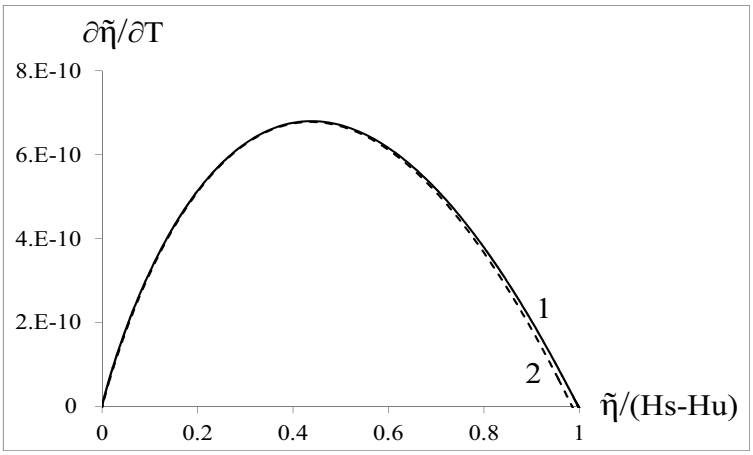

Figure 5: $\partial\widetilde{\eta}/\partial T$ vs $\widetilde{\eta}/(H_s - H_u)$ for $H_s - H_u \ll 1$ at $T = 0$. Line 1 is the numerical solution of the full system, and line 2 is the weakly nonlinear approximation.

and has the form represented by line 1 on Fig. 7 at $X_0 = -20$, then at $T \to \infty$ the front tends to obtain a constant shape and its speed tends to a constant value. At the time $T = 3.45 \cdot 10^6$ (line 2 on Fig. 7) the front speed $W_{full} \approx 1.27 \cdot 10^{-5}$. It is known [3], that under such initial conditions the wave propagation speed determined from equation (14) is equal to 2. In X, Z, T variables, this speed is calculated by the formula

$$W_{KPP} = \frac{2}{3}\frac{\rho_a}{\rho_w}\frac{\nu_a - \nu_*}{\beta}\sqrt{(\beta - \alpha)\left(\frac{\alpha}{{H_u}^2} + \frac{\beta}{(1 - H_u)^2}\right)}.$$

For the case under consideration, $W_{KP} \approx 1.29 \cdot 10^{-5}$. This value is in good agreement with the numerical result shown above.

Note that in this example the condition $(H_s - H_u) \ll H_u$ is not satisfied, so the KPP equation gives a good prediction for the normal front velocity only at $\widetilde{\eta} \ll (H_s - H_u)$. In Fig. 8 the value of $\partial\widetilde{\eta}/\partial T$ is shown. It is obtained in the numerical calculation (line 1) and in the weakly nonlinear approximation. From Fig. 8 it can be seen that good agreement is observed only at $\widetilde{\eta}/(H_s - H_u) < 0.3$. However, this is sufficient for a weakly nonlinear approximation with good accuracy to predict the velocity of the front, since the speed of the front is determined by "tip dynamics", i.e. the dependence of $\widetilde{\eta}$ on X at small $\widetilde{\eta}$.

Therefore, it is seen that the KPP equation predicts many interesting properties that a full system should have. In the next section we concern some stability properties of front solutions of the KPP equation, among them the unknown (to our knowledge) instability of non-positive fronts which may appear in our model. These properties presumably reflect the corresponding behavior of such fronts in the full model.

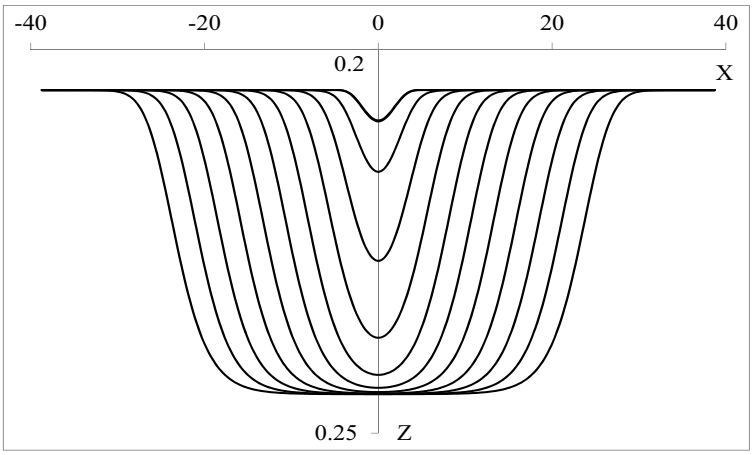

Figure 6: The evolution of the front shape over the time period $\tau \in [0,\, 2.16\,10^6]$.

5. Stability of traveling fronts

Instability of any traveling front solution of (15) may occur because of instability of its right asymptote which is the phase transition interface $\eta = 0$. To see this let us linearize (14) about any traveling wave front solution $\eta_W(\xi)$ and look for the solution $\delta\eta(x,\tau)$ of the linearized equation in the form

$$\delta\eta(x,\tau) = w(\xi)\mathrm{e}^{\lambda\tau}.$$

For $w(\xi)$ we get the equation

$$\begin{aligned} &\mathcal{A}_W w = \lambda w, \\ &\mathcal{A}_W w = w'' + Ww' + \big[1 - 2\eta_W(\xi)\big]w. \end{aligned} \tag{16}$$

From (16) for $\xi \to \pm\infty$ one has $w(\xi) \sim y_\pm(\xi)$,

$$\begin{aligned} 0 &= y_+'' + Wy_+' + (1-\lambda)y_+, \\ 0 &= y_-'' + Wy_-' - (1+\lambda)y_-. \end{aligned} \tag{17}$$

Eq. (17) have solutions $y_\pm = \mathrm{e}^{\mu_\pm\xi}$. The quantities $\mu_\pm$ obey the algebraic equations $P_+(\mu) = 0$ and $P_-(\mu) = 0$, respectively

$$\begin{aligned} P_+(\mu) &= \mu^2 + W\mu + 1 - \lambda, \\ P_-(\mu) &= \mu^2 + W\mu - 1 - \lambda. \end{aligned} \tag{18}$$

For pure imaginary $\mu = \mathrm{i}\kappa$, $\kappa \in \mathbb{R}$ one has

$$\begin{aligned} S^+ &= \{\lambda : \lambda = -\kappa^2 + \mathrm{i}W\kappa + 1\}, \\ S^- &= \{\lambda : \lambda = -\kappa^2 + \mathrm{i}W\kappa - 1\}. \end{aligned}$$

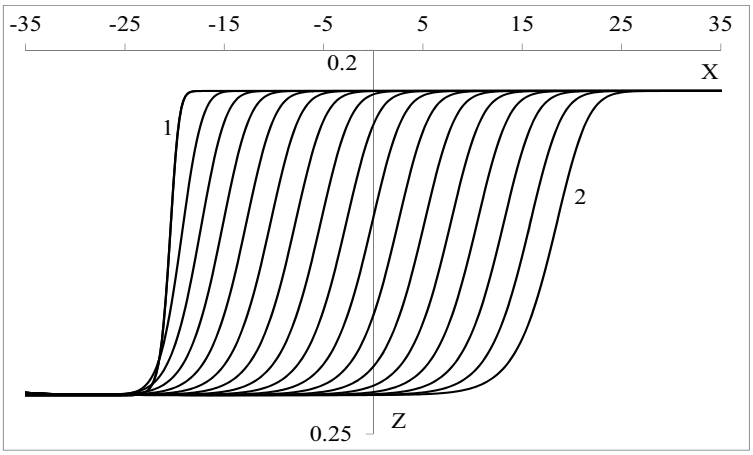

Figure 7: The shapes of the front over the time period $T \in [0,\, 3.45 \cdot 10^6]$.

The set $S^+ \cup S^-$ corresponds to continuous spectrum of the operator $\mathcal{A}_W$ and it interferes in the right half complex λ-plane, which is denoted further by Ω^+, for any $W \geq W_0$ (see Fig. 9). Therefore, we have the following result.

Proposition 4.2. For any $W \geq W_0$ the continuous spectrum of $\mathcal{A}_W$ interferes in Ω^+.

We note, that because of a translational invariance of (14) $\lambda = 0$ is always the eigenvalue of $\mathcal{A}_W$ with the eigenfunction $\eta'_W(\xi)$.

Denote by $\Omega_1^+ \in \Omega^+$ the sub-domain of Ω^+ lying to the right of the curve I in Fig. 9. Further we show that no eigenvalues of $\mathcal{A}_W$ in Ω_1^+ exist.

First we note that from (18) one has

$$\begin{aligned} \mu_{1,2}^+ &= -\frac{W}{2} \pm \sqrt{\frac{W^2}{4} - 1 + \lambda}, \\ \mu_{1,2}^- &= -\frac{W}{2} \pm \sqrt{\frac{W^2}{4} + 1 + \lambda}. \end{aligned} \tag{19}$$

Then, from (19) we have the following statements.

Proposition 4.3. In $\Sigma^+ = \Omega^+ \setminus \Omega_1^+$

$$\operatorname{Re}\mu_1^+ < \operatorname{Re}\mu_2^+ < 0, \quad \operatorname{Re}\mu_1^- < 0 < \operatorname{Re}\mu_2^-.$$

Proposition 4.4. In Ω_1^+

$$\operatorname{Re}\mu_1^\pm < 0 < \operatorname{Re}\mu_2^\pm.$$

We note that in a neighborhood of the curve I in Fig. 4 one has

$$\operatorname{Re}\mu_1^\pm < \operatorname{Re}\mu_2^\pm,$$

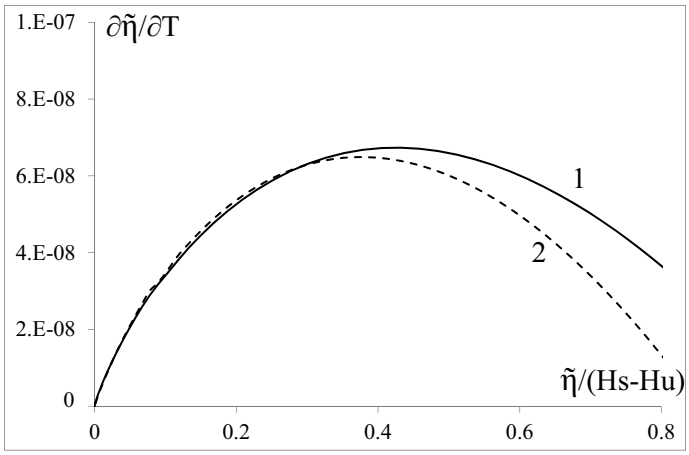

Figure 8: $\partial\widetilde{\eta}/\partial T$ vs $\widetilde{\eta}/(H_s - H_u)$ for moderate $H_s - H_u$ at $T = 3.45 \cdot 10^6$. Line 1 is the numerical solution of the full system, and line 2 is the weakly nonlinear approximation.

therefore $\mu_{1,2}^{\pm}$ are analytic functions in this neighborhood.

Let us rewrite Eq. (16) as the dynamical system

$$\frac{d\mathbf{y}}{d\xi} = \mathbf{A}\mathbf{y}, \quad \mathbf{y} = \{w(\xi,\lambda), w'(\xi,\lambda)\}^{\top},$$
$$\mathbf{A} = \mathbf{A}(\xi,\lambda) = \begin{pmatrix} 0 & 1 \\ -(1-2\eta_w(\xi)-\lambda) & W \end{pmatrix}. \tag{20}$$

Similarly, we have the conjugate system

$$\frac{d\mathbf{z}}{d\xi} = -\mathbf{z}\mathbf{A}, \tag{21}$$

where $\mathbf{z}$ is the two component vector line. The quantities $\mu_i^{\pm}$, $i = 1, 2$ are the eigenvalues of the asymptotic matrices

$$\mathbf{A}^{\pm} = \lim_{\xi\to\pm\infty} \mathbf{A}(\xi,\lambda).$$

Due to Proposition 4.4 there exist the solution $\boldsymbol{\zeta}^{+}(\xi,\lambda)$ of (20) and $\boldsymbol{\eta}^{-}(\xi,\lambda)$ of (21) for $\lambda \in \Omega_1^{+}$ and analytic in λ such that [13]

$$\lim_{\xi\to\infty} \mathrm{e}^{-\mu_1^{+}\xi}\boldsymbol{\zeta}^{+}(\xi,\lambda) = \mathbf{r}(\lambda),$$
$$\lim_{\xi\to-\infty} \mathrm{e}^{\mu_1^{-}\xi}\boldsymbol{\eta}^{-}(\xi,\lambda) = \mathbf{l}(\lambda), \tag{22}$$

where

$$\big(\mathbf{A}^{+} - \mu_1^{+}(\lambda)I\big)\mathbf{r}(\lambda) = 0, \quad \mathbf{l}(\lambda)\big(\mathbf{A}^{-} - \mu_1^{-}(\lambda)I\big) = 0.$$

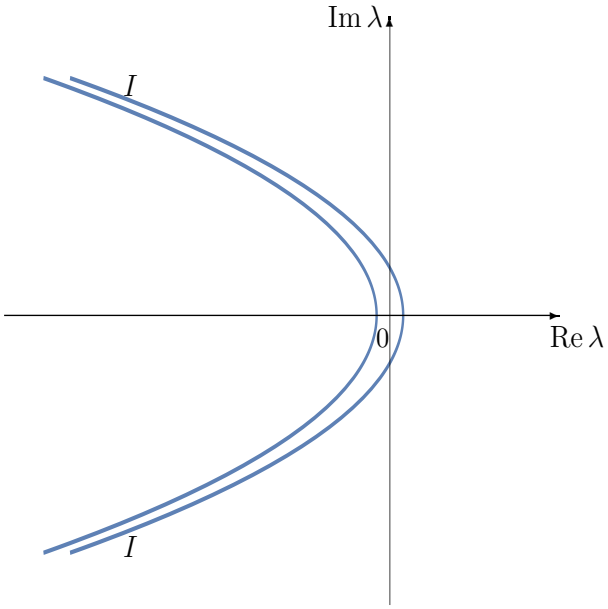

Figure 9: Continuous spectrum of $\mathcal{A}_W$

Analyticity of $\boldsymbol{\zeta}^+(\xi,\lambda)$ and $\boldsymbol{\eta}^-(\xi,\lambda)$ follows from analyticity of $\mu_i^\pm$ for $\lambda \in \Omega_1^+$ (see (19) and arguments of [14]).

A solution of (16) which decays to zero

$$w^+(\xi,\lambda) \sim \exp \mu_1^+ \xi \quad \text{as} \quad \xi \to +\infty$$

for $\lambda \in \Omega^+$. A scattering coefficient $D(\lambda)$, $\lambda \in \Omega_1^+$

$$w^+(\xi,\lambda) \sim D(\lambda) \exp \mu_1^- \xi \quad \text{as} \quad \xi \to -\infty$$

is called Evans function.

Lemma 4.1 [15]. For $\lambda \in \Omega_1^+$ $D(\lambda) = \big(\boldsymbol{\zeta}^+ \cdot \boldsymbol{\eta}^-\big)(\lambda)$ is independent on ξ and analytic in Ω_1^+.

Lemma 4.2 [15, 16]. $D(\lambda) \to 1$ as $|\lambda| \to \infty$.

Lemma 4.3 [15]. $D(\lambda_0) = 0$, $\lambda_0 \in \Omega_1^+$ if and only if there is a solution of (16) which decays exponentially as $\xi \to \pm\infty$, i. e. $\lambda = \lambda_0$ is an eigenvalue of $\mathcal{A}_W$.

The problem of finding the unstable discrete spectrum $\lambda \in \Omega_1^+$ is analogous to determining the zeroes of the Evans function $D(\lambda)$ lying in Ω_1^+. The number of zeroes of $D(\lambda)$ can be computed with the help of the argument principle. The number of zeroes of $D(\lambda)$ in Ω_1^+ is determined by the number of rotations of the image of the left boundary $\partial\Omega_1^+$ of Ω_1^+ under the mapping $D(\cdot)$. Therefore, we need to construct the function $D(\lambda)$ for $\lambda \in \partial\Omega_1^+$, i. e., numerically solve the

ordinary linear equations (20), (21) under the conditions (22) with λ running in a considerably large segment of $\partial\Omega_1^+$. It was shown numerically, that $D(\lambda) \neq 0$ for $\lambda \in \Omega_1^+$. Therefore, we have the following

Theorem 4.1. The discrete spectrum of $\mathcal{A}_W$ is empty in Ω_1^+ for all $W \geq W_0$.

For $\lambda \in \Sigma^+$ both μ_1^+ and μ_2^+ have negative real parts, therefore we have the different situation than for $\lambda \in \Omega_1^+$. In this domain any λ corresponds to an unstable mode destroying a perturbation of our front. Indeed, the asymptotic of any solution of (20) at $\xi \to \infty$ due to Proposition 4.3 has two decaying modes and for $\xi \to -\infty$ it has one decaying mode. Therefore, for any $\lambda \in \Sigma^+$ due to results of [17] there exists the eigenfunction $\boldsymbol{\zeta}^-(\xi, \lambda)$ given by the boundary condition

$$\lim_{\xi \to -\infty} \mathrm{e}^{\mu_2 \xi} \boldsymbol{\zeta}^-(\xi, \lambda) = \mathbf{r}(\lambda).$$

Consequently, we have the following

Theorem 4.2. The solution η_W is linearly exponentially unstable with $\lambda \in \Sigma^+$.

However, the traveling fronts are stable against perturbations decaying appropriately at $\xi \to \infty$.

Definition 4.1. We define the functional space $B_\mu(\mathbb{R})$, $\mu > 0$ as

$$B_\mu(\mathbb{R}) = \{f \in C(\mathbb{R}), ||f||_{B_\mu(\mathbb{R})} < \infty\},$$

where

$$||f||_{B_\mu(\mathbb{R})} = \sup_{\xi \in \mathbb{R}} |f| \mathrm{e}^{\mu \xi}.$$

It can be understood, that we must restrict the decay rate of perturbations when $\xi \to \infty$, i. e. when our front solution tends to its unstable asymptote $\eta = 0$. The weighted space $B_\mu(\mathbb{R})$ is usually used to shift the essential spectrum of the operator in question to the left complex λ half-plane (see, for example, [18]). Since zero still remains the eigenvalue we can speak only about orbital stability of our fronts, or stability in form. Moreover, there is a value of μ where the orbital stability is the asymptotic one, and the following theorem holds.

Theorem 4.3 [19] (see, also [5] and references therein). Let

$$\eta(\xi, 0) = \eta_W(\xi) + \delta\eta(\xi)$$

with $\delta\eta \in B_{W/2}(\mathbb{R})$, $||\delta\eta||_{B_{W/2}(\mathbb{R})}$ is small enough. Then there exist a translation $\theta \in \mathbb{R}$ and constants $K > 0$ and $\nu > 0$ such that

$$||\eta(\cdot, t) - \eta_W(\cdot + \theta)||_{B_{W/2}(\mathbb{R})} = \sup_{\xi \in \mathbb{R}} |\eta(\xi, t) - \eta_W(\xi + \theta)| \mathrm{e}^{W\xi/2} \leq K \mathrm{e}^{-\nu t}$$

holds.

For stable asymptotes the most dangerous perturbations are evidently travel with the front (the case of Theorem 4.3). All other do not have time to develop and the front runs away from them. But when one of these asymptotes is unstable (as in our case) in order the front can run away from stationary perturbations it is necessary that this instability be the convective one in the reference frame firmly connected with a traveling front.

Theorem 4.4 The unstable equilibrium state $\eta = 0$ of (14) is convectively unstable in a coordinate system attached the front solution for $W \geq 2$.

Proof. Equation (14) in the coordinate system firmly attached to the traveling front η_w, i. e. traveling to the left with the speed W takes the form

$$\partial_\tau \eta + W \partial_x \eta = \eta - \eta^2 + \partial^2_{xx} \eta. \tag{23}$$

The dispersion relation for (23) reads

$$-\mathrm{i}\omega = -\mathrm{i}kW + 1 - k^2. \tag{24}$$

From (24) one has that

$$\frac{d\omega(k_0)}{dk} = 0$$

for

$$k_0 = -\mathrm{i}\frac{W}{2}.$$

Therefore

$$\omega(k_0) = \mathrm{i}\left(1 - \frac{W^2}{4}\right),$$

and $\mathrm{Im}\,\omega(k_0) \leq 0$ for $W \geq 2$, i. e. for the range of speeds of existence of monotonous traveling wave front solutions of (14). □

The result of Theorem 4.4 means that linear perturbations of the equilibrium point $\eta = 0$ develop with a speed that is less than $W_0 = 2$.

We now are not restricted to the case when our solution of the KPP equation (14) can be neither greater than one nor smaller than zero. For biological problems and combustion theory problems, only values of $0 \leq \eta \leq 1$ are valid. However, the deviation of the surface of the initially flat front of the phase transition from the equilibrium position can occur not only downwards (in this case $\eta > 0$), but upwards ($\eta < 0$). At the same time, some parts of the front may be below the level of stable equilibrium H_s, so the values $\eta > 1$ are also admissible.

Consequently, we can consider the case $\mathcal{J} = \{W, 0 < W < 2\}$, when the point $\eta = 0$ is a focus. We also can construct heteroclinic structures corresponding to fronts traveling with speeds from this range. They oscillate about the state $\eta = 0$ and tend to it at infinity (examples are given in Fig. 10).

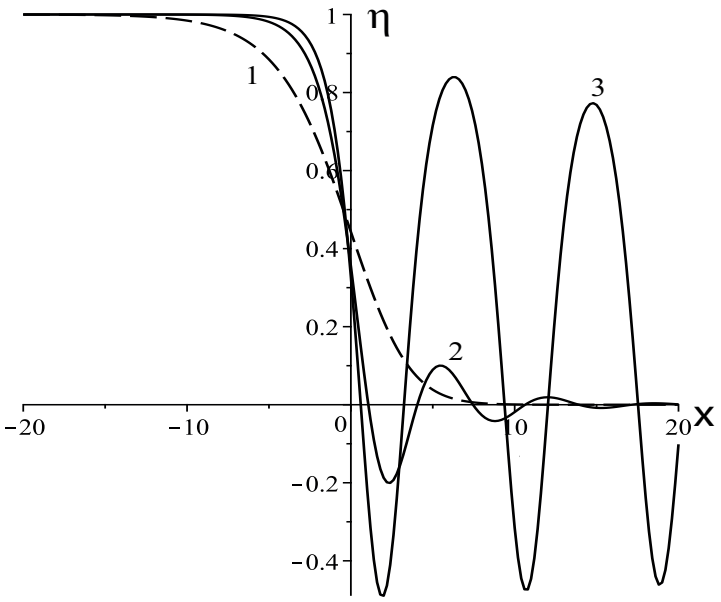

Figure 10: The shape of the traveling wave. 1- $W_{KPP} = 2$, 2- $W_{KPP} = 0.5$, 3 - $W_{KPP} = 0.01$.

According Theorem 4.4. the state $\eta = 0$ is now absolutely unstable, which in its turn means that the fronts with speeds from the range $\mathcal{J}$ are destroyed by corresponding perturbations [20]. There are two scenarios for the development of instability. In the first case, the solution is transformed into a traveling wave, the speed of which asymptotically approaches 2. Such a case is shown in Fig. 11. The initial dependence of the perturbed solution $\eta(x)$ for this calculation was specified as follows

$$\eta = \begin{cases} \eta_{tw}(x) & \text{if } \eta_{tw}(x) \geq 0 \\ 0.99\,\eta_{tw}(x) & \text{if } \eta_{tw}(x) < 0, \end{cases}$$

where $\eta_{tw}(x)$ is the profile of a traveling wave propagating at the speed of W_{KPP}. In the second scenario of instability, a finger is formed, which rapidly increases in amplitude, as shown in Fig. 12. The initial dependence of the perturbed solution $\eta(x)$ for this calculation was specified as follows

$$\eta = \begin{cases} \eta_{tw}(x) & \text{if } \eta_{tw}(x) \geq 0 \\ 1.01\,\eta_{tw}(x) & \text{if } \eta_{tw}(x) < 0. \end{cases}$$

The finger grows up towards the upper bound of the low permeable layer and reaches this bound in finite time.

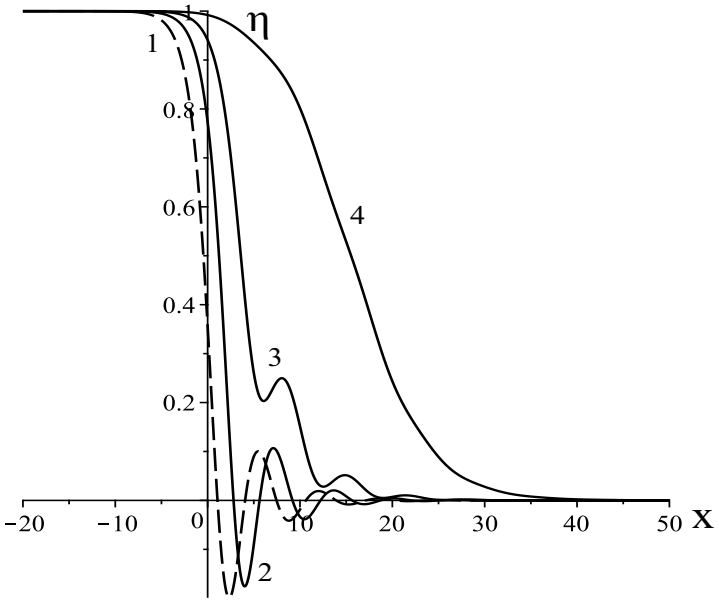

Figure 11: The shapes of the front over the time period $\tau \in [0,\, 10]$. $W_{KPP} = 0.5$.

6. Conclusion and discussion

The present paper is devoted to validity of the model KPP equation in description of phase transition evaporation interfaces in the form of traveling fronts in horizontally extended domains of porous layers where the water is located over the vapor. First, in Sec. 3 it was indicated that for the case of close planar phase transition fronts the dynamics of the system is described by the KPP equation (14). We have shown, that even in case when the plane interfaces are not close and formally we can not use the KPP equation for description of fronts, the maximum deviation of the dimensionless traveling front amplitude from the corresponding (traveling with the same speed) KPP front is small enough. Moreover, the asymptotics of the front at infinity is always described by the KPP equation.

It is known that the KPP equation fronts with monotonous structure (i. e. when the unstable state $\eta = 0$ is a saddle, $W \geq 2$) are asymptotically stable about rapidly decaying perturbations (see Theorem 4.3). (We note in addition, that the various aspects of stability of the KPP-Fischer equations fronts are treated also in [21] and [22]). This, together with small difference of fronts of the full problem from the corresponding fronts of the KPP equation even for finite distance between two plane fronts prompts, that the front dynamics in this case may be described by the KPP equation also for the full problem (3)-(8). Interfaces in the form of front solutions with $W = 2$ arise in dynamics of the system as asymptotics of shapes of localized perturbations of the unstable plane water evaporation surface caused by long-wave instability of vertical flows

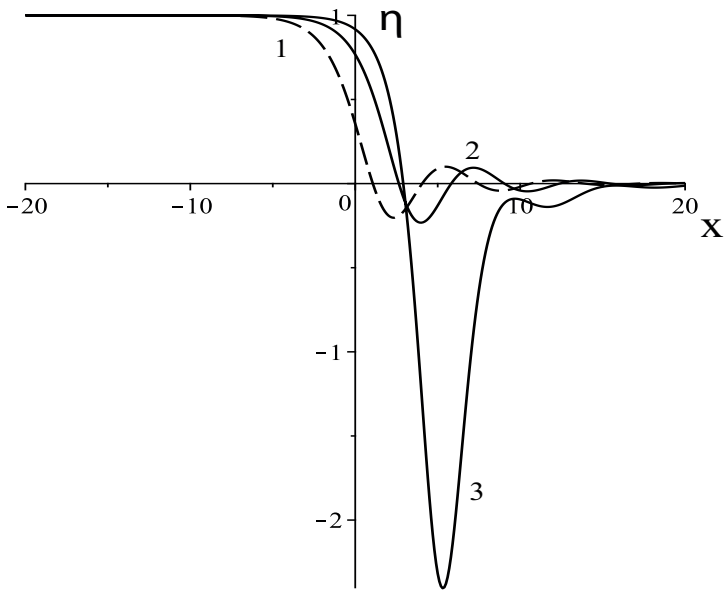

Figure 12: The shapes of the front over the time period $\tau \in [0,\, 6.67]$. $W_{KPP} = 0.5$.

in the non-wettable porous domains.

The properties of the front solutions with monotonous structure of this equation is extensively studied in the literature, though as far as we understand, in the existing still models of population dynamics in one dimensional environment and diffusion-reaction models the consideration is restricted to the domain between two states $\eta = 0$ (which is unstable) and $\eta = 1$ (which is stable). We mention here also the dissertation [23] where this equation is applied to the description of the branching Brownian motion. In our problem we have not no longer such a restriction and therefore, fronts with the oscillating structure also have to be considered. These fronts correspond to heteroclinic interfaces traveling with the speed $W < 2$. Due to results of Theorem 4.4 and the corresponding theory of [20] the front solutions for the case $W < 2$ (i. e. when the unstable state $\eta = 0$ is a focus) are absolutely unstable. Depending on the perturbation it evolves to growing non-stationary state or (which is surprising for us) to the stable front of permanent form propagating with the speed $W = 2$, which serves in this case as an attractor.

Acknowledgment. This work was supported by the Russian Science Foundation, project no. 16-11-10195.

References

[1] G.V. Kolabin, Yu.V. Dyad'kin, V.Zh. Arens, Thermophysical Aspects of Development of Underground Resourses, Nedra:Leningrad, 1988 (in Russian).

[2] A. T. Ilichev and G. G. Tsypkin, Catastrophic transition to instability of evaporation front in a porous medium, *Eur. J. Mech. B Fluids* **27**. 2008. 665-677.

[3] A. N. Kolmogorov, I. G. Petrovskii, and N. S. Piskunov, Study of diffusion equation with an increase in the quantity of matter and its application to a biological problem, *Byull. Mosk. Gos. Univ. Mat. Mekh.* **1** (6). 1937. 1-26.

[4] M. Bramson, Convergence of Solutions of the Kolmogorov Equation to Traveling Waves, *Am. Math. Soc.* Providence, R.I., 1983.

[5] C.J.H. Jonkhout, Traveling wave solutions of reaction-diffusion equations in population dynamics, *Bachelor thesis*. 2016. Mathematical Institute, University of Leiden.

[6] A.T. Il'ichev, V.A. Shargatov, Dynamics of water evaporation fronts, *Computational Math. Math. Phys.* **53**. 2013. 1350–1370.

[7] V.A. Shargatov, A.T. Il'ichev and G.G. Tsypkin, Dynamics and stability of moving fronts of water evaporation in a porous medium, *Int. J. Heat & Mass Transfer* **83**. 2015. 552–561.

[8] D.R. Lide, CRC Handbook of Chemistry and Physics, Boca Raton, New York, Washington, 2001.202.

[9] M.J. Ablowitz, A. Zeppetella, Explicit solutions of Fishers equation for a special wave speed, *Bull. Math. Biology*. **41**. 1979. 835-840.

[10] N.A. Kudryashov, On exact solutions of families of Fisher equations, *Theor. and Math. Phys.* **94**. 1993. 211-218.

[11] J. Berestycki, E. Brunet, B. Derrida, A new approach to computing the asymptotics of the position of Fisher-KPP fronts (2018). http://arxiv.org/abs/1802.03262.

[12] A.T. Il'ichev, G.G. Tsypkin, Instabilities of uniform filtration flows with phase transition, *J. Exp. Theor. Phys.* **107**. 2008. 699–711.

[13] R.L. Pego, M.I. Weinstein, Eigenvalues, and solitary wave instabilities, *Phil. Trans. R. Soc. Lond.* 1992. **A340**. 47–94.

[14] J.C. Alexander, R. Sachs, Linear instability of a Boussinesq-type equation; A computer assisted computation, *Nonlin. World*. 1995. **2**. 471–507.

[15] R.L. Pego, P. Semerka, M.I. Weinstein, Oscillatory instability of traveling waves for a kdvburgers equation, *Physica D*. 1993. **67**. 45–65.

[16] A. T. Il'ichev, A. P. Chugainova, Spectral stability theory of heteroclinic solutions to the Kortewegde Vries-Burgers equation with an arbitrary potential, P̃roc. Steklov Inst. Math. 2016. **295**. 148-157

[17] N. Levinson, The asymptotic nature of solutions of linear systems of differential equations, *Selected Papers of Norman Levinson*. 1998. 1–35.

[18] R.L.Pego, M.I. Weinstein, Asymptotic stability of solitary waves, *Comm. Math. Phys.* 1994. **164**. 305-349.

[19] D. H. Sattinger, On the stability of waves of nonlinear parabolic systems, *Advances in Mathematics*. 1976. **22**. 312–355.

[20] L. Brevdo, Global and absolute instabilities of spatially developing open flows and media with algebraically decaying tails, *Proc. Roy. Soc. Lond. A*. 2003. **459**. 1403–1425.

[21] R. Lui, Existence and stability of traveling wave solutions for an evolutionary ecology model, *Proc. Roy. Soc. Edinburgh A*. 1990. **115**. 1–18.

[22] K. Kirchgässner, On the nonlinear dynamics of traveling fronts, *J. Differ. Equations* **96**. 1992. 256-278.

[23] E. Brunet, Some aspects of the Fisher-KPP equation and the branching Brownian motion, *Thesis of HDR dissertation*. 2016.Sorbonne Universiries.